Politecnico di Torino

Porto Institutional Repository

[Article] New Directions into the Stochastic Geometry Analysis of Dense CSMA Networks

(Article begins on next page)

New Directions into the Stochastic Geometry Analysis of Dense CSMA Networks

Giusi Alfano*, Michele Garetto†, Emilio Leonardi*

* Dipartimento di Elettronica, Politecnico di Torino, Italy

E-mail: {alfano,leonardi}@tlc.polito.it

† Dipartimento di Informatica, Università di Torino, Italy

E-mail: garetto@di.unito.it

Abstract

We consider extended wireless networks characterized by a random topology of access points (APs) contending for medium access over the same wireless channel. Recently, stochastic geometry has emerged as a powerful tool to analyze random networks adopting MAC protocols such as ALOHA and CSMA. The main strength of this methodology lies in its ability to account for the randomness in the nodes' location jointly with an accurate description at the physical layer, based on the SINR, that allows considering also random fading on each link. In this paper we extend previous stochastic geometry models of CSMA networks, developing computationally efficient techniques to obtain throughput distributions, in addition to spatial averages, which permit us to get interesting insights into the impact of protocol parameters and channel variability on the spatial fairness among the nodes. Moreover we extend the analysis to a significant class of topologies in which APs are not placed according to a Poisson process.

Index Terms

CSMA, fairness, random topology, stochastic geometry, general fading

I. INTRODUCTION

The CSMA MAC protocol has become extremely popular nowadays, allowing a large number of users to comfortably enjoy broadband wireless Internet access from their mobile devices (IEEE 802.11). CSMA Access Points (APs) have proliferated in many urban areas, both at public places (airports, train stations, coffee shops, university campuses) and private premises (residential homes, corporate buildings).

The complex behavior of dense CSMA networks, characterized by a large degree of mutual interference among neighboring APs, is still far to be fully understood, making of crucial

importance the availability of analytical models that can predict the impact of the cumulative interference produced by the APs operating over the same channel, by incorporating a realistic description at the physical layer.

Traditional models of CSMA networks typically rely on Markovian approaches. When all terminals are in the sensing range of each other, very accurate and detailed models of 802.11 are available [1]. However Markovian approaches are difficult to apply to large-scale wireless networks employing CSMA, especially if one wants to incorporate the specific details of 802.11 and its impairments (e.g., hidden terminals) [2]. Simplified versions of CSMA are still amenable to Markovian analysis by exploiting the independent sets method originally proposed in [3], which has recently been revisited, coupled with statistical physics arguments, to explain the severe unfairness observed in (regular) heavily loaded networks [4]. However, Markovian models fail to represent physical layer effect (such as the impact of cumulative interference, fading etc.).

From a dual perspective, stochastic geometry has been proposed as a mathematical framework that allows analyzing random, arbitrarily large and arbitrarily dense wireless networks employing variants of ALOHA and CSMA, with an accurate description at the physical layer based on the SINR [5], [6].

The majority of previous work based on the stochastic geometry approach deals with ALOHA networks, whose behavior has been throughly investigated by exact models [7], [8], [9]. CSMA-like networks, unfortunately, cannot be exactly analyzed due to intrinsic difficulties in characterizing the point process of nodes which are allowed concurrently to transmit. In [10] (which is the starting point of our work), the authors proposed a modified Matérn point process to capture key properties of CSMA networks (for Poisson node distribution) while providing a conservative estimate of the transmitters' density. Less conservative hard-core models, such as the Simple Sequential Inhibition [11], [12], turn out to be very challenging to analyze.

In [6, Ch.3] the authors characterize the interference distribution in Poisson networks, both in the absence and in the presence of fading. For CSMA networks, they assume that the interference is produced only by transmitters located outside a disc of radius equal to the sensing range. They also consider the case in which transmitters are distributed according to a Poisson cluster process. The work [13] investigates the optimization of the sensing range in the absence of fading (to maximize the aggregate capacity under the SINR model) for CSMA-like networks where nodes form a Poisson process. In [14] authors develop simple bounds to the outage probability of unslotted ALOHA and CSMA in Poisson networks.

More recently, it has been found that, in the high Signal-to-Interference regime (i.e., when

the density of interferers goes to zero), it is possible to characterize the asymptotic behavior of the outage probability and of the transmission capacity for general isotropic distributions of the transmitters, including the (CSMA-like) Matérn hard-core process [15].

In [16] authors propose a general methodology, based on the factorial expansion of functionals of point processes, that potentially allows estimating (with a controlled degree of approximation) functions of the interference such as the outage probability. The proposed approach is, in principle, fairly general, as it can be applied to a large class of point processs. Nevertheless, in practice, the methodology developed in [16] can be successfully applied only when the n-th order density product of the point process can be efficiently computed.

In [17] stochastic geometric models of channel aware (i.e. opportunistic) versions of CSMA protocol for multi-hop ad-hoc networks have been developed. There, authors provide also a first characterization of the spatial unfairness among the nodes by evaluating the Jain fairness index.

II. PAPER CONTRIBUTION

With respect to previous work, the contribution of our paper is twofold: i) it proposes a methodology to estimate the AP throughput distribution in dense CSMA networks; ii) it defines a computationally efficient procedure to extend the analysis of dense CSMA networks to the case in which APs are not independently placed over the area. For what concerns the first contribution, our work goes in the same direction of the previously cited, parallel effort [17] to characterize the spatial unfairness among the nodes. We emphasize that the throughput distribution obtained in this paper is a more informative metric than the throughput Jain fairness index derived in [17], especially for network design purposes. In this respect, [9] has shown (for dense networks employing ALOHA) that the spatial average of the access delay may become unbounded (through a phase transition) even if the spatial average of the throughput is not null. This effect is caused by strong inhomogeneities among the nodes' throughput: a fraction of the nodes in the network are almost starved, so that their access delay is extremely large, with a dramatic impact on the overall spatial average of the delay. Throughput distributions immediately allow detecting the emergence of starvation, while this is not possible using an aggregate index such as the Jain fairness index.

For the second contribution of our paper, we emphasize that the methodology developed in this paper to tackle cases in which APs are not independently distributed, is complementary to the analysis in [16]. Indeed, [16] proposes a much more general approach that also allows checking the accuracy of the approximation. However, such an approach becomes computation-

ally prohibitive, in practice, when the n-th order density product of the point process can not be easily estimated, for n greater than 2 or 3. This typically occurs in a dense CSMA network in which APs are not independently placed, where statistical properties (such as the n-th order density product) of the point process representing locations of simultaneously transmitting nodes are very complex to characterize. In our work we provide a methodology to analyze a significant class of random topologies in which APs are not independently placed, more precisely, networks in which APs locations must respect a minimum separation degree. This class of topologies is well suited to represent realistic cases in which APs are placed in a coordinated/planned manner (e.g., corporate WLANs, or publicly accessible APs deployed by an Internet Service Provider).

III. NETWORK MODEL

A. Location of Access Points and users

We first assume, similarly to previous work [10], that Access Points (APs) are located according to a homogeneous Poisson point process over the plane with intensity λ_a. This assumption is fairly reasonable when APs are deployed in a fully unplanned fashion, such as in residential scenarios. Indeed, the Poisson assumption implies that, conditionally on the number of APs falling within any bounded network area, these APs are uniformly and independently located over the considered area, which reflects the lack of coordination of unplanned deployment. We denote by $\Phi_A = \{\mathbf{x}_1, \mathbf{x}_2, \ldots \mathbf{x}_k, \ldots\}$ the set of AP locations.

We assume that users are associated with their closest AP. In particular, we suppose that, for each AP, the associated users (we assume there is at least one user per AP) are uniformly distributed within the AP's Voronoi cell.

B. Radio propagation model

We assume that the power received at point $\mathbf{x}$ from a transmitter located at point $\mathbf{y}$, denoted by $P(\mathbf{x}, \mathbf{y})$, is given by $P(\mathbf{x}, \mathbf{y}) = P \cdot l(\mathbf{x}, \mathbf{y}) \cdot F(\mathbf{x}, \mathbf{y})$, where:

- P is the (fixed) transmitted power, common to all APs;
- $l(\mathbf{x}, \mathbf{y})$ is the deterministic component of the path loss between $\mathbf{x}$ and $\mathbf{y}$;
- $F(\mathbf{x}, \mathbf{y})$ is a random variable representing fading and shadowing on the wireless link between $\mathbf{x}$ and $\mathbf{y}$.

We suppose that $l(\mathbf{x}, \mathbf{y})$ depends only on the Euclidean distance $d(\mathbf{x}, \mathbf{y})$ between the transmitter and the receiver. Even if all our expressions hold for a general function $l(d(\mathbf{x}, \mathbf{y}))$, the results that

we will present in this paper are obtained under the following model accounting for near-field effects:

$$l(\mathbf{x}, \mathbf{y}) = \begin{cases} d(\mathbf{x}, \mathbf{y})^{-\alpha} & \text{if } d(\mathbf{x}, \mathbf{y}) > r_0 \\ r_0^{-\alpha} & \text{if } d(\mathbf{x}, \mathbf{y}) \leq r_0 \end{cases} \tag{1}$$

where $r_0 > 0$, and $\alpha > 2$ is the path-loss exponent, which depends on the environment. We will also use the notation $l(r) = (\max(r, r_0))^{-\alpha}$ for all positive real numbers r. The random variables $F(\mathbf{x}, \mathbf{y})$ are assumed to be i.i.d., with generic distribution, for any pair $(\mathbf{x}, \mathbf{y})$[1]. Let $g_F(\zeta)$ be the probability density function of the fading/shadowing random variable, and $\phi_F(s)$ its Laplace transform. We denote by $G_F(\zeta)$ the cumulative distribution function of $g_F(\zeta)$, and by $\bar{G}_F(\zeta) = 1 - G_F(\zeta)$ the complementary of $G_F(\zeta)$.

C. MAC contention model

To determine the subset of APs that transmit simultaneously, we adopt the modified Matérn model proposed in [10], which captures key features of CSMA-like protocols while maintaining analytical tractability. In particular, the model captures the fact that an AP refrains from transmitting when it senses the activity of another AP which has extracted a smaller back-off time. This behavior is modeled in the following way: each point $\mathbf{x}$ of Φ_A is attributed an independent mark $t_{\mathbf{x}}$ uniformly distributed in $[0, 1]$, representing the back-off time. The node transmits if it does not sense the activity of any other node having smaller mark, i.e., nodes that have extracted a shorter backoff. The subset Φ_T of APs transmitting concurrently can be formally defined as

$$\Phi_T = \{\mathbf{x} \in \Phi_A : t_{\mathbf{x}} < t_{\mathbf{y}}, \forall \mathbf{y} : P(\mathbf{x}, \mathbf{y}) > \sigma\}. \tag{2}$$

Notice that, in the absence of fading, set Φ_T becomes a standard hard-core Matérn process with fixed inhibition radius.

The considered MAC contention model ignores collisions, exponential back-off and history of timers. Moreover, it is more suitable to describe the synchronized, slotted version of CSMA, in which nodes independently extract a back-off time at the beginning of a slot, and all concurrent transmissions finish by the end of the slot. The behavior of unslotted, asynchronous CSMA is much more complex, and tends to introduce severe short- and long-term unfairness among the nodes, especially when the average back-off time is much smaller than the packet duration,

---

[1]In the following we will also denote by F the generic marginal random variable $F(\mathbf{x}, \mathbf{y})$.

as in 802.11 (see [4]). Despite its approximate nature, the modified Matérn process provides a conservative, reasonable estimate of the transmitters' density in 802.11 networks, as shown in [10] by comparison with ns2 simulations.

D. Transmission model and throughput analysis

We assume that a transmission is successfully decoded if the SINR at the receiver is larger than a predefined threshold β, which determines the instantaneous rate. We focus on downlink traffic only (i.e., from the APs to the users), assuming, as in previous work, that uplink traffic is negligible. This assumption is justified by the fact that in the current Internet the great majority of the traffic (85%, according to recent measurements in [18]) flows in the downlink direction. Moreover, we assume that APs are constantly backlogged by packets to send. A user located at $\mathbf{x}$ correctly receives data sent by its closest AP at $\mathbf{y}$ when

$$\mathrm{SINR}(\mathbf{x}) = \frac{P(\mathbf{x}, \mathbf{y})}{N_0 + \sum_{\mathbf{j} \in \Phi_T \setminus \mathbf{y}} P(\mathbf{x}, \mathbf{j})} > \beta \tag{3}$$

where N_0 is the (constant) ambient noise power and $I(\mathbf{x}, \mathbf{y}) = \sum_{\mathbf{j} \in \Phi_T \setminus \mathbf{y}} P(\mathbf{x}, \mathbf{j})$ is the cumulative interference produced by all other transmitting APs.

In our throughput analysis we focus on a tagged AP and consider the instantaneous rate $\mathcal{T}$ at which this AP is transmitting at a given time. For simplicity, we will assume that there is exactly one user associated to the tagged AP (i.e., a randomly placed user whose nearest AP is the tagged AP), to avoid the additional complexity of analyzing the bandwidth sharing among users associated to the same AP (i.e., located in the same Voronoi cell). The user throughput can be derived from the AP throughput following the approach proposed in [10].

Moreover, we consider, for simplicity, a unique threshold β, and we normalize to one the corresponding transmission rate. It should be clear, however, that if we are able to evaluate the successful reception probability according to (3), for an arbitrary β, than we can easily compute the throughput achievable with a set of different rates (modulation schemes) selected by an auto-rate function of the SINR (for example, a piecewise constant function).

Under the above assumptions, the instantaneous rate $\mathcal{T}$ of the tagged AP equals the joint probability that: i) the AP is transmitting; ii) the transmission is successfully decoded by the intended receiver. In this paper we are interested both in the spatial average of $\mathcal{T}$ and in its spatial *distribution*.

IV. BASELINE ANALYSIS

In this section we briefly recall the technique proposed in [10] to approximate the spatial throughput average, i.e., the average $\mathbb{E}_0[\mathcal{T}]$ of a tagged AP placed[2] at $\mathbf{0}$, under a Poisson distribution of AP's. In this way we put the reader in a position of understanding our extended analysis. As already shown in [10], in an infinite network the spatial average of the AP's throughput can be confused with the average throughput of a tagged AP placed at the origin, since CSMA protocol rules are by their nature spatially homogeneous, or, in other words, because the pattern of successful transmissions under CSMA does not change when all points are translated on the plane by an arbitrary fixed quantity.

Definition 1: By conditioning on the distance r between the AP and the user, the average AP throughput can be expressed as,

$$\mathbb{E}_0[\mathcal{T}] = \int_0^\infty \mathbb{E}_0[\mathcal{T}|r]\, f_D(r)\, \mathrm{d}r, \tag{4}$$

where $f_D(r)$ is the probability density of the distance between a user and its closest AP, which reads in the Poisson case as

$$f_D(r, \text{Poisson}) = 2\pi r \lambda_a e^{-\lambda_a \pi r^2}. \tag{5}$$

The conditioned average $\mathbb{E}_0[\mathcal{T}|r]$ is given by the product of the conditioned transmission probability $p_T(r)$ of the tagged AP, given that there is a user at distance r (whose closest AP is the tagged AP) and the conditioned probability $p_s(r)$ of successful reception at distance r from the tagged AP, given that this AP transmits.

Hence the computation of the average of the AP throughput requires to evaluate the above defined probabilities $p_T(r)$ and $p_s(r)$.

For what concerns $p_T(r)$, we state the following:

Proposition 1: Let the tagged AP be located at the origin $\mathbf{0}$ (we denote this AP with $\mathbf{0}$ in the following), and the receiving node be located at point $\mathbf{y} = (r, 0)$. We have,

$$p_T(r) = \int_0^1 e^{-\lambda_a t_{\mathbf{0}} \int_{\mathbb{R}^2 \setminus \mathcal{B}(\mathbf{y},r)} S(\mathbf{x})\, \mathrm{d}\mathbf{x}}\, \mathrm{d}t_{\mathbf{0}} = \frac{1 - e^{-\lambda_a \int_{\mathbb{R}^2 \setminus \mathcal{B}(\mathbf{y},r)} S(\mathbf{x})\mathrm{d}\mathbf{x}}}{\lambda_a \int_{\mathbb{R}^2 \setminus \mathcal{B}(\mathbf{y},r)} S(\mathbf{x})\, \mathrm{d}\mathbf{x}}, \tag{6}$$

---

[2]$\mathbb{E}_0[\mathcal{T}]$ should be intended as the Palm expectation operator, which can be intuitively interpreted as the conditional expectation, conditioned on having a node at the origin.

where $\mathcal{B}(\mathbf{y}, r)$ is the ball of radius r centered at $\mathbf{y}$, whereas $S(\mathbf{x})$ is the probability for $\mathbf{0}$ to sense another AP located at $\mathbf{x}$.

Proof: The spatial integral in (6) can be intuitively explained (see [5] for a rigorous proof based on Palm probability and Slivnyak's Theorem) considering that the infinitesimal area $\mathrm{d}\mathbf{x}$ centered at any point $\mathbf{x}$ of the plane (excluding ball $\mathcal{B}(\mathbf{y}, r)$, which by hypothesis does not contain APs) must be free of nodes sensed by $\mathbf{0}$. Conditioning on the mark $t_{\mathbf{0}}$ of AP $\mathbf{0}$ (which provides the outer integral in (6)), the intensity of the Poisson Point process of APs that can potentially prevent $\mathbf{0}$ from transmitting, i.e. those having mark smaller than $t_{\mathbf{0}}$, is $\lambda_a t_{\mathbf{0}}$. This point process is then further thinned by the (location-dependent) probability $S(\mathbf{x})$ that $\mathbf{0}$ indeed senses an AP located at $\mathbf{x}$. We have $S(\mathbf{x}) = \Pr[P(\mathbf{0}, \mathbf{x}) > \sigma] = \bar{G}_F\left(\frac{\sigma}{Pl(x)}\right)$, (where x denotes the euclidean norm $||\mathbf{x}||$) which is the probability that the signal transmitted at $\mathbf{x}$ is received by $\mathbf{0}$ with power above the sensing threshold σ. ∎

To evaluate the probability of successful reception $p_s(r)$, we need to compute (though in an approximate way) the cumulative interference produced by all of the other APs concurrently transmitting with $\mathbf{0}$. For this, we first need an auxiliary function $h(x, \lambda_a)$, which provides the probability that an AP transmits, conditioned on the fact that there is a transmitting AP at distance x from it, belonging to the same Poisson point process of intensity λ_a. Function $h(x, \lambda_a)$ can be evaluated exactly following the approach in [5], which is briefly outlined in Appendix A for the reader's convenience.

Having computed $h(x, \lambda_a)$, we can evaluate in an approximate way the cumulative interference plus noise suffered at the receiving node, by the following:

Lemma 1: Approximating the set of interfering APs with an in-homogenous Poisson point process whose local intensity depends only on the distance x (through function $h(x, \lambda_a)$) from the AP transmitting the useful signal, we can derive an approximation of the Laplace transform $\psi_{I+N_0}(s)$ of interference plus noise as (see [5] for details):

$$\psi_{I+N}(s) = \psi_I(s)\psi_N(s) \approx e^{-\lambda_a \int_0^{2\pi} \int_r^\infty h(b(\rho,\theta),\lambda_a)[1-\phi_F(sPl(\rho))]\rho\,\mathrm{d}\rho\,\mathrm{d}\theta} e^{-sN_0}, \tag{7}$$

where the spatial integral is computed using polar coordinates centered at the receiving node. In this coordinate system, $b(\rho, \theta) = \rho^2 + r^2 - r\rho\cos(\theta)$ provides the distance of the generic point (ρ, θ) from the AP transmitting the useful signal, which is assumed to be located at $(r, 0)$. From the above approximation of the cumulative interference plus noise, we can evaluate the reception probability $p_s(r)$ by the following:

Proposition *2:* For a general fading distribution, we have

$$p_s(r) = \int_0^\infty \bar{G}_F \left(\frac{\beta \xi}{Pl(r)} \right) \mathcal{L}^{-1}\{\psi_{I+N_0}(s)\}|_\xi \, d\xi \,, \tag{8}$$

where we recall that the signal is decoded successfully if the received power exceeds threshold β (see (3)), hence for a given value ξ of $(I + N_0)$, the fading variable F should be larger than $\frac{\beta \xi}{Pl(r)}$.

Expression (8) requires, in general, to numerically invert the Laplace transform $\psi_{I+N_0}(s)$; however, a direct computation of $p_s(r)$ is possible in the special case in which the fading is exponentially distributed (i.e., Rayleigh fading). Indeed, when F is exponential with mean $1/\mu$, we have

$$p_s(r) = \int_0^\infty e^{-\frac{\mu \beta \xi}{Pl(r)}} \, d\Pr(I + N_0 \le \xi), \tag{9}$$

which is equivalent to evaluate the Laplace transform $\psi_{I+N_0}(s)$ at $s = \mu\beta/(Pl(r))$. The expression (9) can be generalized to the case in which the fading variable is phase-type distributed, $G_F(z) = 1 - \sum_i c_i \left(\sum_{k=0}^{K_i} \frac{(\mu_i z)^k}{k!} e^{-\mu_i z} \right)$, with $c_i \ge 0$ and $\sum_i c_i = 1$, obtaining:

$$p_s(r) = \sum_i c_i \left(\sum_{k=0}^{K_i} \int_0^\infty \frac{\gamma_i^k}{k!} e^{-\gamma_i} \, d\Pr(I + N_0 \le \xi) \right), \tag{10}$$

where $\gamma_i = \mu_i \beta \xi/(P\ell(r))$. The computation of (10) reduces to evaluate a linear combination of the Laplace transform $\psi_{I+N_0}(s)$ and its derivatives at points $s_i = \mu_i \beta/(Pl(r))$.

V. BEYOND SPATIAL AVERAGES

In this section we describe how the stochastic geometry approach can be extended to obtain, besides spatial averages, also an estimate of the *distribution* of the throughput achieved by the APs. Doing so, we will get interesting insights into the impact of several system parameters (especially the sensing threshold and the distribution of fading/shadowing) on the discrepancies that we can observe among the throughputs of different APs in a random network. Notice in (4) that we have already identified one cause of variability in the spatial distribution of AP throughput, namely, the one due to the variable distance between an AP and its associated user, which we can account for by the analysis presented so far. Besides the impact of the distance between AP and user, we (separately) capture two additional sources of variability in the spatial

distribution of AP throughput: the variability in the transmission probability $p_T(r)$, in Section V-A, and the variability in the probability $p_s(r)$ of successful reception, in Section V-B. Then in Section V-C we combine everything together obtaining our final estimate of the throughput distribution.

A. Variability in the transmission probability

Clearly, the likelihood of an AP to access the channel is strongly affected by the pattern of contending APs in its neighborhood: even in the presence of fading, the nodes that are most likely to prevent an AP from transmitting are those located in close proximity to it. To capture this fact, we introduce the following:

Proposition 3: The conditional probability $p_T^d(r, n)$ that the tagged AP, located at $\mathbf{0}$, is allowed to transmit, given that there are n other APs within distance d from it (excluding the empty disc of radius r centered at the receiver), is

$$p_T^d(r, n) = \int_0^1 e^{-t_{\mathbf{0}}\mathcal{E}(r,d)}(1 - t_{\mathbf{0}}\mathcal{I}(r, d))^n \, dt_{\mathbf{0}}, \tag{11}$$

where $S(\mathbf{x}) = \bar{G}_F\left(\frac{\sigma}{Pl(x)}\right)$ and

$$\mathcal{E}(r, d) = \lambda_a \int_{\mathbb{R}^2 \setminus (\mathcal{B}(\mathbf{0},d) \cup \mathcal{B}(\mathbf{y},r))} S(\mathbf{x}) \, d\mathbf{x} \qquad ; \qquad \mathcal{I}(r, d) = \frac{\int_{\mathcal{B}(\mathbf{0},d) \setminus \mathcal{B}(\mathbf{y},r)} S(\mathbf{x}) \, d\mathbf{x}}{\int_{\mathcal{B}(\mathbf{0},d) \setminus \mathcal{B}(\mathbf{y},r)} \, d\mathbf{x}}.$$

Proof: Similarly to (6), we condition on the mark $t_{\mathbf{0}}$ associated to AP $\mathbf{0}$. To transmit, the AP must not sense any other AP having smaller mark. The APs located outside the ball $\mathcal{B}(\mathbf{0}, d)$, having mark smaller than $t_{\mathbf{0}}$, form a Poisson process of intensity $\lambda_a t_{\mathbf{0}}$ and can be treated exactly in the same way as before, providing the term $e^{-\lambda_a t_{\mathbf{0}} \mathcal{E}(r,d)}$, which is identical to (6) except for a difference in the spatial integration domain (now we have to exclude two discs from $\mathbb{R}^2$). Then we need to consider the n APs located in the region $\mathcal{B}(\mathbf{0}, d) \setminus \mathcal{B}(\mathbf{y}, r)$, considering that each of them is uniformly distributed in this region, and with probability $t_{\mathbf{0}}$ it has mark smaller than $t_{\mathbf{0}}$. Quantity $\mathcal{I}(r, d)$ provides the probability that the AP senses one of them, considering all possible locations within the region $\mathcal{B}(\mathbf{0}, d) \setminus \mathcal{B}(\mathbf{y}, r)$. Since the AP must not sense any of them, we obtain for this set of nodes the term $(1 - t_{\mathbf{0}} \mathcal{I}(r, d))^n$ in (11). ∎

The parameter d has to be chosen with care: if it is too small, the expected number of APs in $\mathcal{B}(\mathbf{0}, d)$ is also small, and the conditioning becomes ineffective. If it is set large, we loose

control on the number of critical APs (i.e., the nodes most likely to be sensed). A natural choice is to set d equal to the 'effective' sensing range $R_0 = l^{-1}(\sigma/(P\bar{F}))$, which is the fixed inhibition radius of a system in which the fading variable is deterministically equal to its mean.

B. Variability in the probability of successful reception

The probability of successful reception $p_s(r)$ at distance r from the AP is strongly affected by the pattern of interferers around the receiver, as well as on the characteristics of the wireless channel (i.e., path loss exponent, and fading/shadowing distribution). Proceeding in a similar way as for the transmission probability, we state the following:

Proposition 4: The conditional probability $p_s^e(r, m)$ of successful reception, given that there are m transmitting APs within distance e from the receiver, with $e > r$ (by construction there are no APs at distance smaller than r) can be obtained according to (8), (9), (10), respectively for general, Rayleigh or phase type fading distribution, once the Laplace transform on the corresponding conditional interference plus noise distribution is given.

Under our assumptions on nodes locations, $\psi_{I+N_0}^e[r, m](s) =$

$$
= e^{-\lambda_a \int_0^{2\pi} \int_e^\infty h(b(\rho,\theta),\lambda_a)[1-\phi_F(sPl(\rho))]\rho \, d\rho \, d\theta} \left(\frac{\int_0^{2\pi} \int_r^e h\left(b(\rho,\theta),\lambda_a\right) \phi_F(sPl(\rho))\rho \, d\rho \, d\theta}{\int_0^{2\pi} \int_r^e h\left(b(\rho,\theta),\lambda_a\right) \rho \, d\rho \, d\theta} \right)^m e^{-sN_0}.
$$

(12)

Proof: By definition the cumulative interference at the receiver is the sum of all powers received from transmitting APs other than the good one. The corresponding Laplace transform is the product of the Laplace transform of the individual contributions. The contribution of APs located outside the disc of radius e centered at the receiver can be treated exactly in the same way as before, providing the first exponential term in (12), which is identical to (7) except for the different integration domain. Note that we are using polar coordinates centered at the receiver, with the transmitter located at $(r, 0)$.

Then we need to consider the m APs located in the region $\mathcal{B}(\mathbf{0}, e) \setminus \mathcal{B}(\mathbf{0}, r)$, considering that each of them is located at point (ρ, θ) with density proportional to the local intensity $\lambda_a h\left(b(\rho, \theta), \lambda_a\right)$ of the inhomogeneous Poisson process of APs concurrently transmitting. Hence the contribution of each of the m APs is

$$
\frac{\int_0^{2\pi} \int_r^e h\left(b(\rho,\theta),\lambda_a\right) \phi_F(sPl(\rho))\rho \, d\rho \, d\theta}{\int_0^{2\pi} \int_r^e h\left(b(\rho,\theta),\lambda_a\right) \rho \, d\rho \, d\theta}.
$$

Considering also the contribution of the ambient noise, we get the expression in (12).   ∎

Again, parameter e has to be chosen with care, trying to isolate those APs which are responsible for the highest variability in the interference. In our results we have set $e = 1.5r$, which has empirically been found to provide the best fit with simulations.

C. Throughput distribution

Definition *2:* In analogy with previous section and former definition of conditioned AP throughput (4), we introduce the spatial average of the conditioned throughput $\mathbb{E}_0[\mathcal{T}|n, m, r]$ of a tagged AP, located at $\mathbf{r}$, transmitting to a user located at the origin $\mathbf{0}$, given that there are n other APs within the area $\mathcal{B}(\mathbf{r}, d) \setminus \mathcal{B}(\mathbf{0}, r)$ and m other APs in the ring $\mathcal{B}(\mathbf{0}, e) \setminus \mathcal{B}(\mathbf{0}, r)$:

$$\mathbb{E}_0[\mathcal{T}|r, n, m] = p_T^d(r, n) p_s^e(r, m). \tag{13}$$

At last we obtain our estimated law for the spatial distribution of $\mathcal{T}$ by combining together all considered sources of variability, as stated in the following:

Proposition *5:* An estimate of the AP throughput distribution can be expressed as:

$$\mathbb{P}\{\mathcal{T} < \eta\} \approx \sum_n \sum_m \int_0^\infty \mathbf{1}_{(\mathbb{E}_0[\mathcal{T}|r,n,m]<\eta)} F_r^{d,e}(n, m) f_D(r) \, \mathrm{d}r.$$

Proof: Denoting by $\mathcal{A}_r^d$ the area of region $\mathcal{B}(\mathbf{r}, d) \setminus \mathcal{B}(\mathbf{0}, r)$, the probability $F_r^d(n)$ to find n other APs in it is

$$F_r^d(n) = e^{-\lambda_a \mathcal{A}_r^d} \frac{(\lambda_a \mathcal{A}_r^d)^n}{n!}$$

Instead, the probability $F_r^e(n)$ to find m other transmitting APs in the ring $\mathcal{B}(\mathbf{0}, e) \setminus \mathcal{B}(\mathbf{0}, r)$ is

$$F_r^e(m) \approx e^{-\lambda_a \int_0^{2\pi} \int_r^e h(b(\rho,\theta), \lambda_a) \rho \, \mathrm{d}\rho \, \mathrm{d}\theta} \frac{(\lambda_a \int_0^{2\pi} \int_r^e h(b(\rho, \theta), \lambda_a) \rho \, \mathrm{d}\rho \, \mathrm{d}\theta)^m}{m!}.$$

The joint probability $F_r^{d,e}(n, m)$ to find n APs in region $\mathcal{B}(\mathbf{r}, d) \setminus \mathcal{B}(\mathbf{0}, r)$ and m APs in region $\mathcal{B}(\mathbf{0}, e) \setminus \mathcal{B}(\mathbf{0}, r)$ can be approximated as

$$F_r^{d,e}(n, m) \approx F_r^d(n) F_r^e(m),$$

where the approximation lies in the fact that the above two regions are non disjoint, thus the numbers of points falling in them are not independent. From the given expression for $F_r^{d,e}(n, m)$, the throughput law approximation follows.

We emphasize that, in principle, a more accurate estimate of $F_r^{d,e}(n, m)$ can be obtained by conditioning on the number of nodes k lying in the intersection of regions $\mathcal{B}(\mathbf{r}, d) \setminus \mathcal{B}(\mathbf{0}, r)$ and $\mathcal{B}(\mathbf{0}, e) \setminus \mathcal{B}(\mathbf{0}, r)$. This refinement, however, comes at a cost of a significant increase in the model computational complexity.

D. AP throughput distribution: results and insights

In this subsection we report a selection of the most interesting results that can be obtained following our approach to estimating the spatial distribution of AP throughput. Since our formulas contain several approximations, model predictions are checked against results obtained by a Montecarlo simulator of the system as described in Section III. The spatial integrals of our approximate analysis are computed numerically using standard discretization methods.

We remark that our approximation becomes asymptotically tight in the following two asymptotic regimes: 1) when the sensing threshold $\sigma \to 0$; 2) when the density of APs $\lambda_a \to 0$. In the first regime, indeed, throughput performance is dominated by the transmission probability, which is exactly characterized in our model (under the simplifying description of the pattern of CSMA transmitters as a Matérn point process); In the second regime, the second-order product density $(\lambda_a h(x, \lambda_a))$ used in the model to approximately describe the pattern of interfering APs becomes asymptotically exact, when $\lambda_a \to 0$. This because, for any finite domain $\mathcal{O}$, the probability that three or more points lie within $\mathcal{O}$ becomes negligible with respect to the probability of having 2 points.

In all presented cases we will assume that $P = 1$, $\beta = 1$. Unless otherwise specified, we will consider the path-loss exponent $\alpha = 3$. Furthermore, we will assume that $N_0 = 0$, i.e., we will focus on interference-limited networks, in which the impact of the ambient noise power is negligible.

1) **Impact of sensing threshold on the spatial average of AP throughput:** before exploring throughput distributions, it is interesting to look at how the spatial average $\mathbb{E}_0[\mathcal{T}]$ of the AP throughput depends on the sensing threshold σ, that governs the transmission probability (6) through the sensing function $S(\mathbf{x}) = \Pr[P(\mathbf{0}, \mathbf{x}) > \sigma]$ (see baseline analysis in Section IV). Indeed, it was such preliminary observation that motivated us to look at spatial distributions instead of just spatial averages.

We consider a scenario in which APs are placed according to a Poisson process with intensity $\lambda_a = 1/\pi$, while fading is exponentially (Rayleigh) distributed with mean $1/\mu = 1$.

Fig. 1 reports the spatial average $\mathbb{E}_0[\mathcal{T}]$, the (de-conditioned) transmission probability $p_T = \int_0^\infty p_T(r) f_D(r) \, \mathrm{d}r$ and the (de-conditioned) probability of successful reception $p_s = \int_0^\infty p_s(r) f_D(r) \, \mathrm{d}r$, as function of the sensing threshold σ. Model predictions turn out to be rather accurate in the considered scenario, despite the several approximations (for the throughput figure we have also reported 99%-level confidence intervals derived from our simulations).

As expected, the transmission probability p_T increases with σ (since the probability to sense nearby nodes and thus refrain from transmitting decreases), whereas the success probability p_s decreases with σ (since there is more interference). The overall effect on average throughput is instead less obvious: AP throughput increases with σ up to a maximum value. Beyond this point the throughput decreases very little as we further augment σ (a similar behavior occurs for different values of α and β). Recall that we assume that users are always associated to the closest AP (the decay of the throughput after the optimum value can be more pronounced under different user-AP association models).

Looking just at Fig. 1, one would be tempted to conclude that in dense CSMA networks the sensing mechanism is not that useful (at least under the closest-AP user association). Indeed observe that an aloha-like protocol[3] would achieve nearly maximum throughput. However, the spatial average of AP throughput provides alone a limited view of the system behavior, and here is exactly where our approach to estimating the throughput distribution comes into play to better understand the role of sensing.

2) **Impact of sensing threshold on AP throughput distribution:** Fig. 2 reports the estimated cumulative distribution function (cdf) of the AP throughput (14) for three values of $\sigma = 0.1, 1, 10$.

We observe that the *sensing threshold has a dramatic impact on the spatial fairness among the nodes*. Indeed, for large values of σ a significant fraction of APs (those in more unfavorable topological conditions) experience negligible throughput (starvation), being their transmissions systematically affected by strong interference. *Reducing σ (i.e., increasing the sensing range) permits evening out the throughput of contending APs*, at the cost of a reduction in the average AP throughput (Fig. 1). Although capacity-fairness trade-offs are common in many communication systems, ours is probably the first analytical model to show such trade-off within the stochastic geometry framework to analyze random CSMA networks. We observe that our approach to estimating the throughput distribution well predicts the impact of of σ, although it tends to underestimate the lower tail of the distribution (see Fig. 2). This because our approach is able

---

[3]As σ tends to infinity, the system behaves like slotted-Aloha with transmit probability equal to 1.

to capture the main sources of variability in the throughput distribution, but cannot estimate precisely the occurrence of rare topological conditions leading to extremely low throughput.

3) **Impact of fading variability on AP throughput distribution:** another interesting effect that can be captured by our analysis is related to the shape of the fading/shadowing variable. In Fig. 3 we show again the cdf reported in 2 in the case of $\sigma = 10$, which was shown to produce a severe unbalance in the throughput distribution under Rayleigh fading. This time, we increase the variation coefficient of the fading/shadowing variable (while maintaining the same mean), considering second order hyper-exponential distributions instead of a simple exponential. In the first hyper-exponential case, labelled "hyper–A", we consider a combination of two exponentials of means $\mu_1 = 1/3$, $\mu_2 = 3$ (moderate variation coefficient). In the second hyper-exponential case, labelled "hyper–B", we consider a combination of two exponentials of means $\mu_1 = 1/10$, $\mu_2 = 10$ (large variation coefficient).

We observe that *higher diversity in the fading distribution increases the spatial fairness, alleviating the starvation of APs in unfavorable topological conditions*. This again occurs at the expense of a reduction in the average AP throughput (not shown here). The model captures fairly well this counter-intuitive phenomenon.

We considered also the case of fading distributions which do not allow a phase-type representation. In this case, one approach to evaluate the reception probability is to numerically invert the Laplace transform of interference and noise (8), which can be, however, computationally expensive. Alternatively, we have found that a phase-type distribution matching the first few moments of the original distribution provides in general satisfactory result, especially with respect to the other forms of approximation introduced in the analysis. As an example, we have considered the case of log-normal fading, which is sometimes used to model the amplitude change in signal caused by shadowing. We recall that a log-normal distribution has variation coefficient (v.c.) $\sqrt{e^{v-1}}$, where v is the variance of the normal distribution which is obtained by taking the logarithm of the log-normal random variable. While maintaining the mean of the log-normal distribution equal to one, we have investigated different values of v.c. considering $v = \log 2$ (which correspond to a v.c. equal to 1), $v = 1$, $v = 2$. Then we have fitted each considered log-normal distribution by an hyper-exponential distribution of the second order, which allows matching the first three moments of the corresponding log-normal distribution. The resulting cdf's of AP throughput, as obtained by simulation, are reported in Fig. 4, in the case of $\sigma = 10$. We observe that the cdf resulting from the fitted hyper-exponential distributions (which can be estimated also analytically) are close to the corresponding ones resulting from

the log-normal distribution. We conclude that a limited phase-type representation allows obtaining satisfactory results also for general (possibly long-tailed) fading distributions, while more complex approaches would produce only marginal improvements.

4) **Impact of path-loss exponent on AP throughput distribution:** at last in Fig. 5 we investigate the impact on the path-loss exponent α on the throughput distribution, restricting our attention to Rayleigh fading and $\sigma = 1$. As expected, smaller values of α increase the aggregate amount of interference in the network, resulting in much smaller throughputs. Besides this, our analysis also captures the fact that, *for small values of the path-loss exponent, the throughput distribution is largely unbalanced,* (see the curve labelled $\alpha = 2.1$) with a significant fraction of nodes experiencing negligible throughput (about 20% of the nodes achieve less than 0.01 throughput). Indeed, in this case the node performance is more susceptible to local topological conditions (i.e., network areas more or less populated by nodes). For large values of α, instead, the impact of unfavorable topological conditions is mitigated, thus the spatial fairness increases. We can also observe that in the considered scenario the average throughput increases with α. This apparently surprising result should be taken with care, since we have assumed that the ambient noise power is negligible ($N_0 = 0$). When this is not the case, the average throughput is not monotonic with α, since for very large power attenuation the network performance becomes noise-limited.

We conclude this part summarizing our main findings, reminding that our insights have been obtained under the closest-AP user association policy:

- increasing the sensing range of CSMA improves the spatial fairness in the network, but reduces the average throughput;
- for increasing variability of the fading distribution (keeping fixed the mean), the spatial fairness in the network improves, while the average throughput decreases;
- for increasing path-loss exponent, the spatial fairness in the network improves, as well as the average throughput, as long as the network is interference-limited (i.e., the ambient noise is negligible).

VI. BEYOND THE POISSON PROCESS

Usually in planned networks APs are not placed independently of each other[4]. Hence the Poisson point process is not well suited to describe controlled network topologies. In particular,

---

[4]this is true also in unplanned networks, e.g., residential APs, although in a weaker sense.

in the Poisson point process we can find nodes arbitrarily close to each other, which is something that any reasonable strategy of nodes placement tries to avoid. To minimize mutual interference, while maximizing area coverage, the optimal solution would be to place the APs according to a regular tessellation of the plane (e.g., a triangular lattice). However, APs cannot in general be deployed at any location, due to physical and cost constraints. Hence some randomness in the AP topology has to be considered. To reflect the above facts, we model the point process of APs by a hard-core Matérn process of parameters (λ, R), which guarantees a minimum separation constraint of R between APs. Notice that this model can also be used to represent, in unplanned scenarios, the repulsive effect induced by intelligent channel selection schemes, or, in the context of green networking, the effect of switching off redundant APs covering the same region of the network area. Fig. 6 shows a portion of a sample topology generated by a Matérn process with parameters $\lambda = 10/\pi$, $R = 1$. Note that there are no nodes separated by a distance smaller than $R = 1$.

In this section we will show that the above Matérn model of AP placement can be smoothly incorporated in the previous analysis, resorting to the same Poisson approximation for the intensity of the (conditioned) Matérn process. We proceed as follows. In Section VI-A we compute the conditional transmission probability $p_T(r)$ of an AP, given that there is a user at distance r from it. In Section VI-B we evaluate the probability of successful reception $p_s(r)$ at the user.

At last, to finally apply the throughput formula (4), we need to estimate the distribution $f_D(r, \text{Matérn})$ of the distance r between the AP and the user. In the case of a (hard-core) Matérn process of APs, such distribution is not known in closed form. Therefore we have developed an approximate analysis of $f_D(r, \text{Matérn})$ which is sufficiently accurate for our purposes. The details of this analysis can be found in Sect. VI-C.

A. Transmission probability

Similarly to what has been done before to characterize the set of transmitting APs, we first characterize the set of AP locations by computing the probability $g(x, \lambda, R)$ that, given the existence of an AP in the origin, we find another AP at distance x from it. We start by the following

Lemma 2: Let Φ be the set of 'candidate' AP locations generated by the original Poisson point process of rate λ, and let $\mathbb{P}_\Phi^{0,\mathbf{x}}\{\}$ be the probability law associated with point process

$\Phi + \mathbf{0} + \mathbf{x}$. The desired function

$$g(x, \lambda, R) = \mathbb{P}^{\mathbf{0},\mathbf{x}}_{\Phi}\{\mathbf{x} \in \Phi_A \mid \mathbf{0} \in \Phi_A\}$$

can be expressed[5], by specializing (20) to the case of no fading (we consider now a hard-core Matérn process), in closed form as

$$g(x, \lambda, R) = \mathbf{1}(x > R)\frac{2}{1 - e^{-\lambda\pi R^2}}\left[\frac{1 - e^{-\lambda(\pi R^2 + M(x))}}{\lambda(\pi R^2 + M(x))} - e^{-\lambda\pi R^2}\frac{1 - e^{-\lambda M(x)}}{\lambda M(x)}\right],$$

where $M(x)$ is the area of $\mathcal{B}(\mathbf{x}, R) \setminus \mathcal{B}(\mathbf{0}, R)$, illustrated in Fig. 7 by a light gray region. ¿From the above result, it is straightforward to show that

Proposition 6: The conditional transmission probability $p_T(r)$ for the case in which APs are placed according to an inhomogeneous Poisson process reads as:

$$p_T(r) = \int_0^1 e^{-t_{\mathbf{0}} \int_{\mathbb{R}^2 \setminus \mathcal{B}(\mathbf{y}, r)} \lambda_a^0(\mathbf{x}) S(\mathbf{x})\,\mathrm{d}\mathbf{x}}\,\mathrm{d}t_{\mathbf{0}}, \tag{14}$$

once we approximate the law $\lambda_a^0(\mathbf{x})$ of Φ_A, conditioned on the event $\mathbf{0} \in \Phi_A$, by an inhomogeneous Poisson point process of intensity

$$\lambda_a^0(\mathbf{x}) = \lambda\, g(x, \lambda, R). \tag{15}$$

B. Probability of successful reception

To evaluate the probability of successful reception $p_s(r)$, we need to characterize the set of APs transmitting concurrently with the tagged AP located at $\mathbf{0}$. The key step consists again in computing function $h(x, \lambda, R) = \mathbb{P}^{\mathbf{0},\mathbf{x}}_{\Phi_A}\{\mathbf{x} \in \Phi_T \mid \mathbf{0} \in \Phi_T\}$, which can be interpreted as the conditional probability that AP $\mathbf{x} \in \Phi_A$ transmits, given that AP $\mathbf{0} \in \Phi_A$ is transmitting. Function $h(x, \lambda, R)$ can then be used to characterize (in an approximate way) the law of transmitting APs around AP $\mathbf{0}$. The computation of $h(x, \lambda, R)$ can be carried out by approximating the law of the other APs (different from $\mathbf{x}$ and $\mathbf{0}$) with an inhomogeneous Poisson process of intensity $\lambda_a^{\mathbf{0},\mathbf{x}}(\mathbf{z}) = \lambda\,\mathbb{P}^{\mathbf{0},\mathbf{x},\mathbf{z}}_{\Phi}\{\mathbf{z} \in \Phi_A \mid \mathbf{0} \in \Phi_A, \mathbf{x} \in \Phi_A\}$, where $\mathbb{P}^{\mathbf{0},\mathbf{x},\mathbf{z}}_{\Phi}\{\}$ is the probability law associated to the point process $\Phi + \mathbf{0} + \mathbf{x} + \mathbf{z}$. Function $h(x, \lambda, R)$ can then be computed by extending (21)

---

[5]Notice that $g(x, \lambda, R)$ can be evaluated in a way analogous to function $h(x, \lambda_a)$ in (20) (see Appendix A), although with a very different meaning (here we are characterizing the set of APs location, not yet the set of transmitting APs).

and (22) to the case of an in-homogeneous Poisson process of intensity $\lambda_a^{0,x}(z)$. In particular, (21) becomes:

$$\mathbb{P}_{\Phi_A}^{0,x}\{x \in \Phi_T, 0 \in \Phi_T\} = 2G_F\left(\frac{\sigma}{Pl(x)}\right)\int_0^1\int_{t_0}^1 e^{-(t_x-t_0)\int_{\mathbb{R}^2}\lambda_a^{0,x}(z)S_x(z)\,dz}\,dt_x e^{-t_0\int_{\mathbb{R}^2}\lambda_a^{0,x}(z)S_{0\,\text{or}\,x}(z)\,dz}\,dt_0,$$

(16)

and similarly for (22):

$$h(x,\lambda,R) \approx \frac{2\left[\bar{G}_F\left(\frac{\sigma}{P\ell(x)}\right)\right]}{\mathbb{P}_{\Phi_A}^{0,x}\{0 \in \Phi_T\}}\int_0^1\int_{t_0}^1 e^{-(t_x-t_0)\int_{\mathbb{R}^2}\lambda_A^{0,x}(z)S_x(z|t_0<t_z<t_x)\,dz}\,dt_x$$

$$e^{-t_0\int_{\mathbb{R}^2}\lambda_A^{0,x}(z)S_{0\,\text{or}\,x}(z|t_z<t_0)\,dz}\,dt_0,$$

where

$$\mathbb{P}_{\Phi_A}^{0,x}\{0 \in \Phi_T\} \approx \int_0^1\left\{\int_0^{t_x} e^{-t_0\int_{\mathbb{R}^2}\lambda_A^{0,x}(z)S_0(z|t_z<t_0)\,dz}\,dt_0+\right.$$

$$\left.\int_{t_x}^1\left[\bar{G}\left(\frac{\sigma}{P\ell(x)}\right)\right]e^{-t_0\int_{\mathbb{R}^2}\lambda_A^{0,x}(z)S_0(z|t_z<t_0)\,dz}\,dt_0\right\}\,dt_x.$$

To compute $\lambda_a^{0,x}(z)$, we extend the approach used to derive (15) to the case of three points, obtaining

$$\lambda_a^{0,x}(z) = \lambda\,\mathbb{P}_\Phi^{0,x,z}\{z \in \Phi_A \mid 0 \in \Phi_A, x \in \Phi_A\} = \lambda\frac{\mathbb{P}_\Phi^{0,x,z}\{z \in \Phi_A, 0 \in \Phi_A, x \in \Phi_A\}}{\mathbb{P}_\Phi^{0,x,z}\{0 \in \Phi_A, x \in \Phi_A\}} =$$

$$= \lambda\frac{6\,\mathbb{P}_\Phi^{0,x,z}\{z \in \Phi_A, 0 \in \Phi_A, x \in \Phi_A \mid t_z<t_x<t_0\}}{2\,\mathbb{P}_\Phi^{0,x,z}\{0 \in \Phi_A, x \in \Phi_A \mid t_x < t_0\}} =$$

$$= 3\lambda\frac{\int_0^1\int_{t_z}^1\int_{t_x}^1 e^{-\lambda t_0\pi R^2}e^{-\lambda t_x M(x)}e^{-\lambda t_z N(x,z)}\,dt_0\,dt_x\,dt_z}{\int_0^1\int_{t_x}^1 e^{-\lambda t_0\pi R^2}e^{-\lambda t_x M(x)}\,dt_0\,dt_x},$$

which can be computed in closed form as function of the area $M(x)$ of $\mathcal{B}(x,R)\setminus\mathcal{B}(0,R)$, and of the area $N(x,z)$ of $\mathcal{B}(z,R)\setminus(\mathcal{B}(x,R)\cup\mathcal{B}(0,R))$, illustrated in Fig. 7 by a light gray region and a dark gray region, respectively.

Given that we approximately describe the process of transmitting APs around AP 0 as an inhomogeneous Poisson process of intensity $\lambda_a^0(x)h(x,\lambda,R)$, we can easily obtain the characteristic function of the cumulative interference adapting (8):

$$\psi_I(s) = e^{-\int_0^{2\pi}\int_0^r \lambda_a^0(b(\rho,\theta))h(b(\rho,\theta),\lambda,R)[1-\phi_F(sPl(\rho))]\rho\,\mathrm{d}\rho\,\mathrm{d}\theta}, \tag{17}$$

where we remind that the spatial integrals are computed using polar coordinates centered at the receiving node, being $b(\rho,\theta)$ the distance of the generic point (ρ,θ) from the AP transmitting the useful signal. The success probability $p_s(r)$ can finally be obtained plugging $\psi_{I+N}(s) = \psi_I(s)e^{-sN_0}$ in (8), (9), and (10), respectively for general, Rayleigh or phase type fading distribution.

At last we wish to emphasize that our Matérn model of AP locations can be extended to evaluate also throughput distributions, following the same approach outlined in Section V, which essentially requires to replace λ_A with $\lambda_A^0(x)$ and $h(z,\lambda_A)$ with $h(z,\lambda,R)$ in (11) and (12).

C. Distance distribution between transmitter and receiver.

We need to evaluate the distance distribution between a node n arbitrarily placed on the plane and the closest AP belonging to Φ_A (denoted with A). When Φ_A is a standard Poisson process, the above distribution is well known (5). Unfortunately, instead, when Φ_A is a (hardcore) Matérn point process, the above distance distribution is (to the best of our knowledge) not known in closed form. Therefore we approximate it with a form similar to (5), which provides an estimate of $f_D(r, \text{Matérn})$ sufficiently accurate for our purposes. Our approximation is based on a simple observation, which allows modifying (5) adapting it to the case of a Matérn process of parameters (λ, R). The observation is that, for all values r such that $2r \leq R$, the exact probability $f_D(r, \text{Matérn})$ is

$$f_D(r, \text{Matérn}) = 2\pi r\lambda p, \qquad \text{for} \quad 2\,r \leq R, \tag{18}$$

where $p = \frac{1-e^{-\lambda\pi R^2}}{\lambda\pi R^2}$ is the probability of retaining a point in the original Poisson point process. Indeed, consider the case $2r \leq R$ illustrated in the left part of Fig. 11. Once we know that there is a point $A \in \Phi_A$ at distance $d \in [r, r + \mathrm{d}r]$ (this event has probability $2\pi r\lambda p\,\mathrm{d}r$), we do not need to worry about the presence of other APs closer to n than A (i.e., other nodes belonging to Φ_A, lying within the disk of radius r centered at n). Indeed, when $2r \leq R$ this disk is entirely contained in the disk of radius R centered at A, which by definition cannot contain any other point belonging to Φ_A.

Instead, in the case $2r > R$, we need to worry about the possible presence of APs closer to n than A, but only in the area denoted by a shaded region in the right part of Fig. 11. Our approximation is to assume that the existence of these closer APs depends uniquely on the area $M(r, R)$ of the region where we can find them. The value of $M(r, R)$ can be computed in closed form applying elementary geometry, and we omit its expression here. Moreover, we assume that nodes belonging to Φ_A populate area $M(r, R)$ with a probability equivalent to that of a virtual Poisson point process of intensity λ^*. Hence we write

$$f_D(r, \text{Matérn}) \approx 2\pi r \lambda p e^{-\lambda^* M(r,R)}, \tag{19}$$

which is valid also for $2r \leq R$, assuming that $M(r, R) = 0$ in this case. At last, the value of λ^* to be used in (19) is the only one that guarantees that $f_D(r, \text{Matérn})$ is a proper pdf, i.e., it is the unique value λ^* such that $\int_0^\infty 2\pi r \lambda p e^{-\lambda^* M(r,R)} \, \mathrm{d}r = 1$. We have found that this simple approximation provides sufficiently accurate distributions for all values of λ and R.

D. Matérn process of APs: results and insights

In this subsection, we evaluate the effect of different APs placements on the average AP throughput and its spatial distribution.

1) **Impact of minimum AP separation on average throughput:** Fig. 8 reports the spatial average $\mathbb{E}_0[\mathcal{T}]$ as function of the average density $\bar{\lambda}$ of APs in the network, in the case of Rayleigh fading with $\sigma = 1$. Besides the Poisson process (for which $\bar{\lambda} = \lambda_a$), we consider hard-core Matérn processes (λ, R) with different radius R, in which we let λ vary from very small to very large values, obtaining average node densities $\bar{\lambda} = \frac{1 - e^{-\lambda \pi R^2}}{\pi R^2}$. We observe that, *for given average node density $\bar{\lambda}$, the average AP throughput increases with the minimum AP separation R (but notice that R cannot exceed $1/\sqrt{\pi\bar{\lambda}}$).* This effect can be explained by the fact that the resulting topologies become more and more regular, with a beneficial effect also on the distance distribution between AP and user. What is somehow surprising is that, *for fixed minimum AP separation R, the average AP throughput can even increase for increasing values of the AP's density*, if R is sufficiently large (see curves related to $R = 0.75, 1, 2$). This can be again attributed to the fact that, for a given R, Matérn processes become more regular by increasing λ (and $\bar{\lambda}$), although this beneficial effect can be offset, for small R, by the increased interference. We observe, again, that our model is able to capture fairly well this interesting phenomenon.

2) **Impact of path-loss exponent on average throughput:** in Fig. 9 we explore the impact of the path-loss exponent α in the case of a Matérn process of APs with $R = 1$, focusing again on Rayleigh fading with $\sigma = 1$. For a given α, the AP throughput slightly increases when AP density increases, as confirmed by both simulation and analysis. We again observe that the average throughput increases with α, but this unexpected behavior depends on the fact that we have assumed an interference-limited system, in which the impact of the ambient noise is negligible ($N_0 = 0$).

3) **Impact of sensing threshold on AP throughput distribution:** at last, Fig. 10 reports the throughput cdf for a fixed Matérn process with $\lambda = 10/\pi$ and $R = 1$. We consider Rayleigh fading, and different values of the sensing threshold $\sigma = 0.1, 1, 10$. We have also reported the throughput cdf's for the cases in which AP's form a Poisson process with same average AP density. We observe that, *besides increasing the average AP throughput (see Fig. 8), a more regular placement of the APs with respect to the Poisson process is also able to reduce throughput variability*, as correctly predicted by the model.

In summary, a careful deployment of APs can significantly improve the average throughput performance as well as reduce the spatial unfairness among APs.

VII. CONCLUSIONS

In this paper we have extended the stochastic geometry approach to modeling dense CSMA networks. So far, spatial averages of performance measures have provided only a limited, possibly misleading view of the system behavior, and therefore they must be supplemented with an analysis of the spatial distribution of the same measures. We have shown how the stochastic geometry analysis can provide fundamental insights into the throughput distribution, especially how the inherent unbalance due to the randomness in the topology is affected by the sensing mechanism and the variability of radio signal propagation. Moreover, we have proposed a methodology that permits us to consider scenarios in which APs are not distributed according to a Poisson process, obtaining additional insights that could guide the topology design and control of densely deployed CSMA networks.

REFERENCES

[1] G. Bianchi, "Performance analysis of the IEEE 802.11 distributed coordination function," *IEEE JSAC*, vol. 18, pp. 235–247, 2000.

[2] M. Garetto, T. Salonidis, and E.-W. Knightly, "Modeling per-flow throughput and capturing starvation in CSMA multi-hop wireless networks," *IEEE/ACM Trans. Netw.*, vol. 16, no. 4, pp. 864–877, 2008.

[3] R. Boorstyn, A. Kershenbaum, B. Maglaris, and V. Sahin, "Throughput analysis in multihop CSMA packet radio networks," *IEEE Transactions on Communications*, vol. 35, pp. 267–274, 1987.

[4] M. Durvy, O. Dousse, and P. Thiran, "On the fairness of large CSMA networks," *IEEE JSAC*, vol. 27, pp. 1093–1104, 2009.

[5] F. Baccelli and B. Błaszczyszyn, "Stochastic geometry and wireless networks, vol. 2: Applications," *Foundations and Trends in Networking*, vol. 4, no. 1-2, pp. 1–312, 2009.

[6] M. Haenggi and R. K. Ganti, "Interference in Large Wireless Networks," *Foundations and Trends in Networking*, Vol. 3, no. 2, pp. 127–248, 2009.

[7] F. Baccelli, B. Błaszczyszyn, and P. Mühlethaler, "An aloha protocol for multihop mobile wireless networks," *IEEE Transactions on Information Theory*, vol. 52, no. 2, pp. 421–436, 2006.

[8] F. Baccelli, B. Błaszczyszyn, and P. Mühlethaler, "A stochastic model for spatial and opportunistic aloha," *IEEE JSAC*, vol. 27, no. 7, pp. 1105–1119, 2009.

[9] F. Baccelli and B. Błaszczyszyn, "A New Phase Transition for Local Delays in MANETs," *In Proc. IEEE INFOCOM 2010*.

[10] H. Q. Nguyen, F. Baccelli, and D. Kofman, "A Stochastic Geometry Analysis of Dense IEEE 802.11 Networks," *IEEE INFOCOM 2007*.

[11] A. Busson and G. Chelius, "Point processes for interference modeling in CSMA/CA ad-hoc networks," *PE-WASUN 2009*.

[12] I. Palasti, "On some random space filling problem," *Publ. Math. Inst. Hung. Acad. Sci.*, vol. 1, no. 5, pp. 353–359, 1960.

[13] A. Hasan and J. Andrews, "The guard zone in wireless ad hoc networks," *IEEE Trans. on Wireless Comm.*, 6(3), pp. 897–906, 2007.

[14] M. Kaynia, G. E. Øien, and N. Jindal, "Impact of fading on the performance of ALOHA and CSMA," *SPAWC 2009*.

[15] R. K. Ganti, J. G. Andrews, and M. Haenggi, "High-SIR Transmission Capacity of Wireless Networks with General Fading and Node Distribution," *IEEE Trans. on Information Theory*, vol.57, no.5, pp.3100-3116, May 2011.

[16] R, K. Ganti, F. Baccelli, J. G. Andrews, "Series Expansion for Interference in Wireless Networks", submitted to IEEE Trans. on Information Theory, 2011; available on-line at: http://arxiv.org/abs/1101.3824.

[17] Y. Kim, F. Baccelli and G. de Veciana, "Spatial Reuse and Fairness in Mobile Ad-Hoc Networks With Channel-Aware CSMA Protocols", submitted to IEEE Trans. on Information Theory, 2011; available on-line at: http://users.ece.utexas.edu/~gustavo/publications.php.

[18] G. Maier, A. Feldmann, V. Paxson, and M. Allman, "On dominant characteristics of residential broadband internet traffic," *IMC '09*.
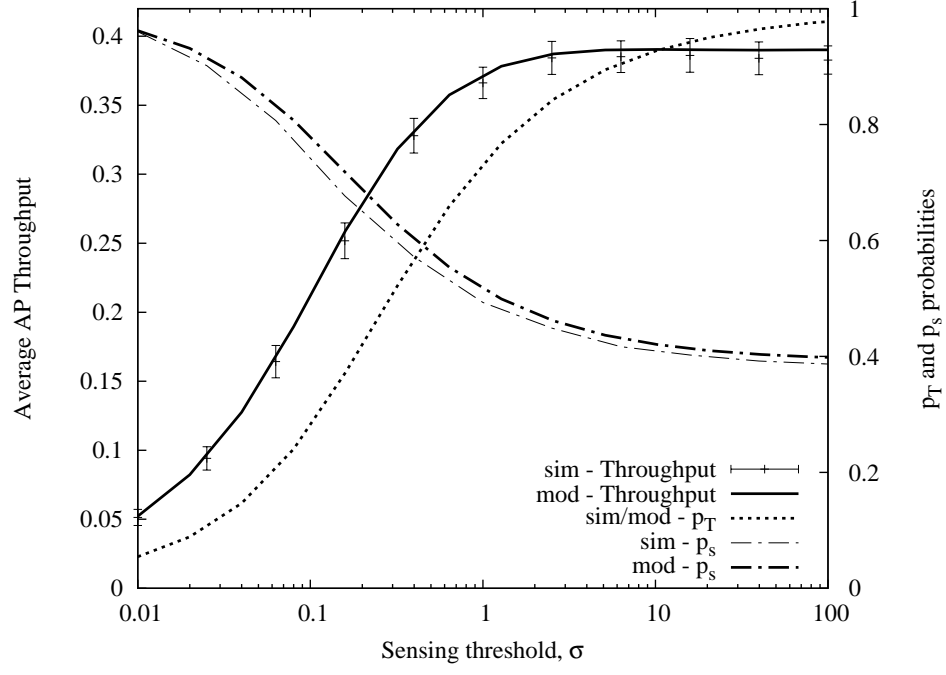
Fig. 1.   Spatial average of AP throughput (left y axis), average transmission probability p_T and average success probability p_s (right y axis), as function of the sensing threshold σ, for $\lambda_A = 1/\pi$, Rayleigh fading.
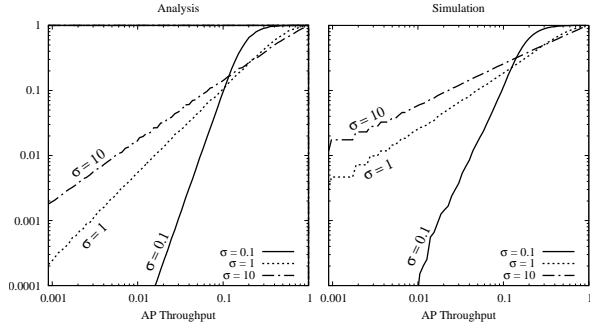
Fig. 2. CDF of AP throughput, for different values of the sensing threshold σ, in the same scenario as of Fig. 1. Comparison between analysis and simulation.
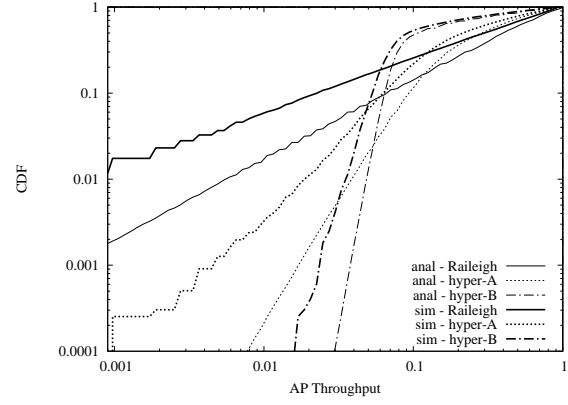

Fig. 3. CDF of AP throughput, for different distributions of fading/shadowing, in the case of $\sigma = 10$, $\lambda_A = 1/\pi$. Comparison between analysis and simulation.
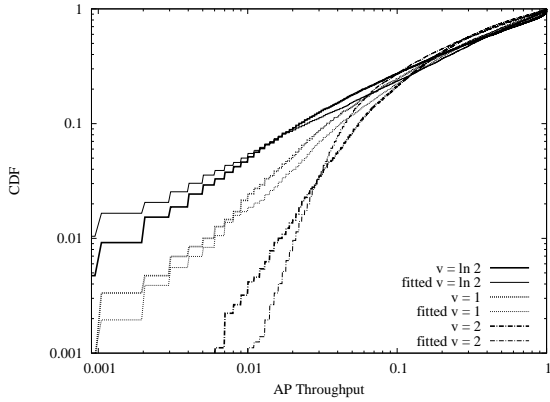

Fig. 4. CDF of AP throughput, obtained by simulation in the case of $\sigma = 10$, $\lambda_A = 1/\pi$. Comparison between log-normal distributions and their fitted hyper-exponentials of the second order.
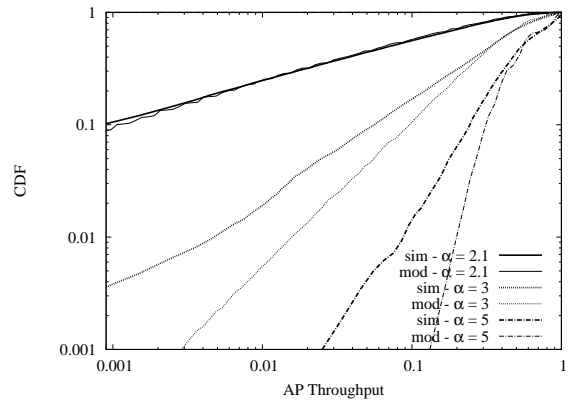

Fig. 5. CDF of AP throughput, for different values of α, in the case of $\sigma = 1$, $\lambda_A = 1/\pi$, Rayleigh fading. Comparison between analysis and simulation.
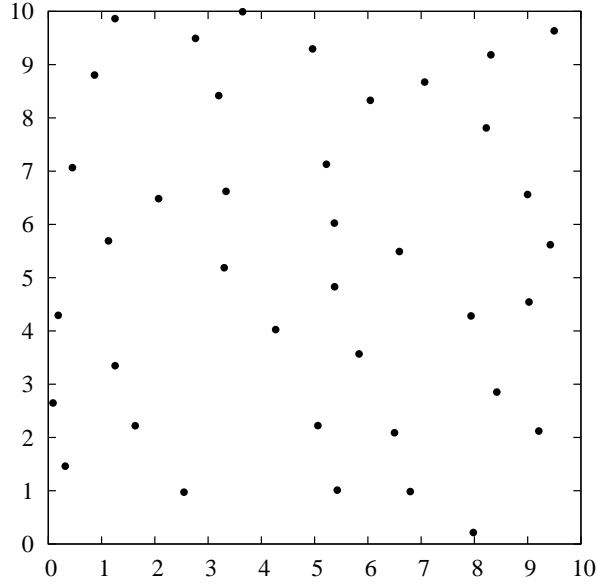
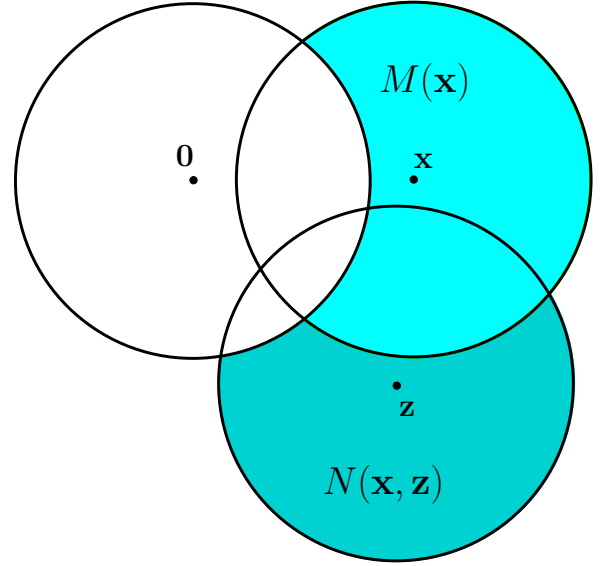Fig. 6. Example of topology generated by a Matérn process with $\lambda = 10/\pi$, $R = 1$.

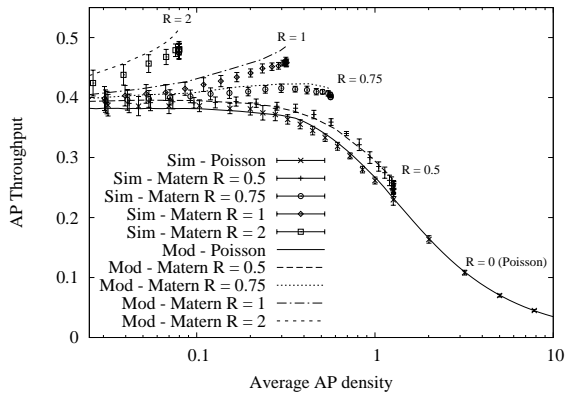Fig. 7. Geometry used to compute joint/conditional probabilities of node patterns in the Matérn process.

Fig. 8. Average AP throughput as function of the (average) AP density λ_a, for different point processes of APs, in the case of $\sigma = 1$, Rayleigh fading.
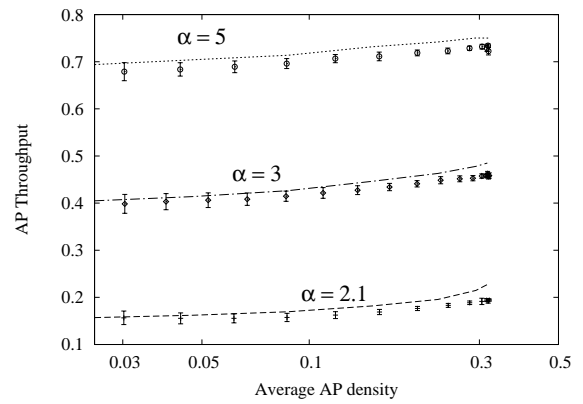

Fig. 9. Average AP throughput as function of the (average) AP density λ_a, for different values of α, in the case of a Matérn process with $R = 1$, $\sigma = 1$, Rayleigh fading.
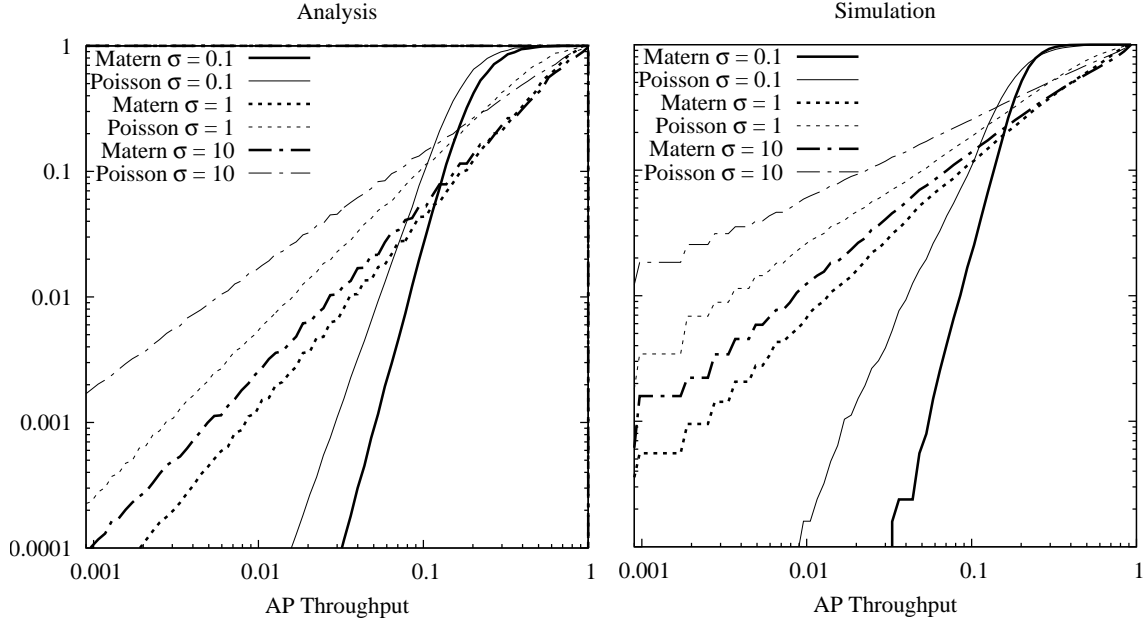
Fig. 10. CDF of AP throughput, for different values of the sensing threshold σ, in the case of a Matérn process with $R = 1$, $\lambda = 10/\pi$, and the corresponding Poisson (with the same AP density), for Rayleigh fading. Comparison between analysis (left plot) and simulation (right plot).
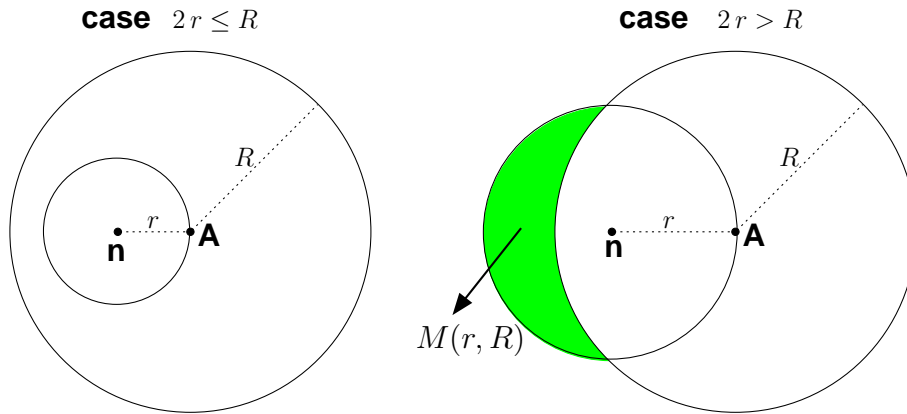

Fig. 11. Illustration of the two cases arising in the approximate computation of the distance distribution between a node n and its closest Access Point A, in the case of a Matérn process of APs.

Giusi Alfano Giusi Alfano was born in Naples, Italy, on march 22, 1978. She received Laurea degree in Communication Engineering from University of Naples Federico II, Italy, in 2001. From 2002 to 2004 she was involved in radar and satellite signal processing studies at National Research Council and University of Naples. In October 2007 she graduated as ph.d. in Information Engineering at University of Benevento, Italy. She was post-doc at Politecnico di Torino, Italy, from 2008 to 2012, periodically visiting ftw Wien, Supélec Paris and NTNU Trondheim. Her research work lies mainly in the field of random matrix theory applications to MIMO wireless communications and sensor networks, and to the characterization of physical layers of random networks.

Michele Garetto (S'01–M'04) received the Dr.Ing. degree in Telecommunication Engineering and the Ph.D. degree in Electronic and Telecommunication Engineering, both from Politecnico di Torino, Italy, in 2000 and 2004, respectively. In 2002, he was a visiting scholar with the Networks Group of the University of Massachusetts, Amherst, and in 2004 he held a postdoctoral position at the ECE department of Rice University, Houston. He is currently assistant professor at the University of Torino, Italy. His research interests are in the field of performance evaluation of wired and wireless communication networks.

Emilio Leonardi (M'99) received the Dr.Ing degree in electronics engineering and the Ph.D. degree in telecommunications engineering from the Politecnico di Torino, Torino, Italy, in 1991 and 1995, respectively. He is currently an Associate Professor in the Department of Electronics, Politecnico di Torino. In 1995, he was with the Department of Computer Science, University of California at Los Angeles. In the summer of 1999, he was with the High Speed Networks Research Group, Lucent Technology-Bell Labs, Holmdel, NJ, and in the summer of 2001, he was with the Department of Electrical Engineering, Stanford University, Stanford, CA. He has coauthored over 100 papers published in international journals and presented in leading international conferences. His areas of interest are all-optical networks, queueing theory, and scheduling policies for high-speed switches.

APPENDIX A

COMPUTATION OF FUNCTION $h(x, \lambda_a)$.

Let $\mathbf{0}$ and $\mathbf{x}$ be two APs at distance x from each other, and let $t_{\mathbf{0}}$ and $t_{\mathbf{x}}$ be their marks. We can express $h(x, \lambda_a)$ as

$$h(x, \lambda_a) = \mathbb{P}_{\Phi_A}^{\mathbf{0},\mathbf{x}}\{\mathbf{x} \in \Phi_T \mid \mathbf{0} \in \Phi_T\} = \frac{\mathbb{P}_{\Phi_A}^{\mathbf{0},\mathbf{x}}\{\mathbf{x} \in \Phi_T, \mathbf{0} \in \Phi_T\}}{\mathbb{P}_{\Phi_A}^{\mathbf{0},\mathbf{x}}\{\mathbf{0} \in \Phi_T\}}, \tag{20}$$

where $\mathbb{P}_{\Phi_A}^{\mathbf{0},\mathbf{x}}\{\}$ is the probability law associated to the point process $\Phi_A + \mathbf{0} + \mathbf{x}$; observe that $\mathbb{P}_{\Phi_A}^{\mathbf{0},\mathbf{x}}\{\mathbf{x} \in \Phi_T, \mathbf{0} \in \Phi_T\}$ is the probability that two APs placed at distance x from each other transmit concurrently, whereas $\mathbb{P}_{\Phi_A}^{\mathbf{0},\mathbf{x}}\{\mathbf{0} \in \Phi_T\}$ is the probability that $\mathbf{0}$ transmits, given that there is another AP at distance x from it (not necessarily concurrently transmitting).

We start computing the joint probability that $\mathbf{0}$ and $\mathbf{x}$ transmits concurrently. When considering all possible combinations of $t_{\mathbf{x}}$ and $t_{\mathbf{0}}$, we can limit ourselves to the case $t_{\mathbf{0}} < t_{\mathbf{x}}$, and then multiply the result by two (the case $t_{\mathbf{x}} < t_{\mathbf{0}}$ is symmetric). Besides nodes $\mathbf{0}$ and $\mathbf{x}$, we need to consider the superposition of two independent homogeneous Poisson point processes: a process of intensity $\lambda_a t_{\mathbf{0}}$, related to those nodes having mark $t < t_{\mathbf{0}}$ that can be sensed by nodes $\mathbf{0}$ and/or node $\mathbf{x}$; a process of intensity $\lambda(t_{\mathbf{x}} - t_{\mathbf{0}})$, related to those nodes having mark $t_{\mathbf{0}} < t < t_{\mathbf{x}}$ that can be sensed by node $\mathbf{x}$ only. Hence we can express $\mathbb{P}_{\Phi_A}^{\mathbf{0},\mathbf{x}}\{\mathbf{x} \in \Phi_T, \mathbf{0} \in \Phi_T\}$ as

$$\mathbb{P}_{\Phi_A}^{\mathbf{0},\mathbf{x}}\{\mathbf{x} \in \Phi_T, \mathbf{0} \in \Phi_T\} = 2\, G_F\left(\frac{\sigma}{Pl(x)}\right) \int_0^1 \int_{t_{\mathbf{0}}}^1 e^{-\lambda_a(t_{\mathbf{x}} - t_{\mathbf{0}}) \int_{\mathbb{R}^2} S_{\mathbf{x}}(\mathbf{z})\, \mathrm{d}\mathbf{z}}\, \mathrm{d}t_{\mathbf{x}} e^{-\lambda_a t_{\mathbf{0}} \int_{\mathbb{R}^2} S_{\mathbf{0}\,\text{or}\,\mathbf{x}}(\mathbf{z})\, \mathrm{d}\mathbf{z}}\, \mathrm{d}t_{\mathbf{0}}. \tag{21}$$

In the above equation, the term $G_F\left(\frac{\sigma}{Pl(x)}\right)$ corresponds to the probability that the AP transmitting first is not sensed by the other, which is the only requirement to have the two nodes concurrently transmitting when there are no other nodes in the network; $S_{\mathbf{x}}(\mathbf{z})$ is the probability that node $\mathbf{x}$ senses a node at $\mathbf{z}$; $S_{\mathbf{0}\,\text{or}\,\mathbf{x}}(\mathbf{z}) = 1 - (1 - S_{\mathbf{0}}(\mathbf{z}))(1 - S_{\mathbf{x}}(\mathbf{z}))$ is the probability that at least one node (between $\mathbf{0}$ and $\mathbf{x}$) senses a node at $\mathbf{z}$.

The conditional probability $\mathbb{P}_{\Phi_A}^{\mathbf{0},\mathbf{x}}\{\mathbf{0} \in \Phi_A\}$ can be obtained in a similar way, this time considering all possible combinations of $t_{\mathbf{0}}$ and $t_{\mathbf{x}}$:

$$\mathbb{P}_{\Phi_A}^{\mathbf{0},\mathbf{x}}\{\mathbf{0} \in \Phi_T\} = \int_0^1 \left\{ \int_0^{t_{\mathbf{x}}} e^{-\lambda_a t_{\mathbf{0}} \int_{\mathbb{R}^2} S_{\mathbf{0}}(\mathbf{z})\, \mathrm{d}\mathbf{z}}\, \mathrm{d}t_{\mathbf{0}} + \int_{t_{\mathbf{x}}}^1 G_F\left(\frac{\sigma}{Pl(x)}\right) e^{-\lambda_a t_{\mathbf{0}} \int_{\mathbb{R}^2} S_{\mathbf{0}}(\mathbf{z})\, \mathrm{d}\mathbf{z}}\, \mathrm{d}t_{\mathbf{0}} \right\} \mathrm{d}t_{\mathbf{x}}. \tag{22}$$

In the above expression, $G_F\left(\frac{\sigma}{Pl(x)}\right)$ is the probability that $\mathbf{0}$ does not sense the transmission of $\mathbf{x}$, when $t_{\mathbf{0}} > t_{\mathbf{x}}$.